Biogeosciences, 4, 853–868, 2007
www.biogeosciences.net/4/853/2007/

Biogeosciences

Relationship between photosynthetic parameters and different proxies of phytoplankton biomass in the subtropical ocean

Y. Huot[1], **M. Babin**[1], **F. Bruyant**[2], **C. Grob**[4], **M. S. Twardowski**[3], **and H. Claustre**[1]

[1]CNRS, Laboratoire d'Océanographie de Villefranche, 06230 Villefranche-sur-Mer, France; Université Pierre et Marie Curie-Paris 6, Laboratoire d'Océanographie de Villefranche, 06230 Villefranche-sur-Mer, France
[2]Dalhousie University, Department of Oceanography, 1355 Oxford Street, Halifax N.S. B3H 4J1, Canada
[3]WET Labs, Inc., Department of Research, 165 Dean Knauss Dr., Narragansett, RI 02882, USA
[4]Graduate Program in Oceanography, Department of Oceanography and Center for Oceanographic Research in the eastern South Pacific, University of Concepción, Casilla 160-C, Concepción, Chile

Received: 20 February 2007 – Published in Biogeosciences Discuss.: 1 March 2007
Revised: 7 September 2007 – Accepted: 22 September 2007 – Published: 16 October 2007

Abstract. Probably because it is a readily available ocean color product, almost all models of primary productivity use chlorophyll as their index of phytoplankton biomass. As other variables become more readily available, both from remote sensing and in situ autonomous platforms, we should ask if other indices of biomass might be preferable. Herein, we compare the accuracy of different proxies of phytoplankton biomass for estimating the maximum photosynthetic rate ($P_{\max}$) and the initial slope of the production versus irradiance (P vs. E) curve (α). The proxies compared are: the total chlorophyll *a* concentration (Tchl*a*, the sum of chlorophyll *a* and divinyl chlorophyll), the phytoplankton absorption coefficient, the phytoplankton photosynthetic absorption coefficient, the active fluorescence in situ, the particulate scattering coefficient at 650 nm (b_p (650)), and the particulate backscattering coefficient at 650 nm (b_{bp} (650)). All of the data (about 170 P vs. E curves) were collected in the South Pacific Ocean. We find that when only the phytoplanktonic biomass proxies are available, b_p (650) and Tchl*a* are respectively the best estimators of $P_{\max}$ and α. When additional variables are available, such as the depth of sampling, the irradiance at depth, or the temperature, Tchl*a* is the best estimator of both $P_{\max}$ and α.

Correspondence to: Y. Huot
(huot@obs-vlfr.fr)

1 Introduction

Photosynthesis (P) in the ocean can be conveniently described using two basic quantities: the phytoplankton biomass (B), and the photosynthetic rates per unit biomass P^{B}; $P{=}B\,P^{\mathrm{B}}$. Both quantities can be measured in situ and are highly variable. To obtain global estimates of productivity, however, these quantities must be estimated for all oceans and with sufficient temporal resolution and this cannot be achieved by shipboard sampling. Because phytoplankton absorption changes the color of the light leaving the ocean, B can be obtained accurately using satellite imagery (using chlorophyll *a* as a proxy). Since P^{B} cannot be measured on large scales continuously, an alternative method must be used to estimate it. Finding an appropriate method has proven difficult. Indeed, despite years of research, its estimate remains the largest uncertainty in our models of oceanic primary production.

The main variable influencing P^{B} is the incident irradiance. Describing this influence is relatively simple as it can be mathematically represented by a saturating function (Falkowski and Raven, 1997): the so-called PvsE curve. This function can be parameterized using two parameters: α^{B} [usually mgC (mgChl)$^{-1}$ h^{-1} (μmol photon m^{-2} s^{-1})$^{-1}$] which describes the initial slope; and $P^{\mathrm{B}}_{\max}$ [usually mgC (mgChl)$^{-1}$ h^{-1}] which describes the amplitude of the light-saturated plateau. If $P^{\mathrm{B}}_{\max}$ and α^{B} are known, the influence of incident light on P^{B} is known. The most difficult aspect is the prediction of variability in $P^{\mathrm{B}}_{\max}$ and α^{B} that originates from changes in the physiological state (i.e.

Published by Copernicus Publications on behalf of the European Geosciences Union.

photoacclimation and nutritional status) of phytoplankton or in the species composition of the community.

On the one hand, it has long been observed that if $P^{\mathrm{B}}_{\mathrm{max}}$ is normalized to carbon (B=carbon), $P^{\mathrm{B}}_{\mathrm{max}}$ is almost independent of the growth irradiance, reflecting a parallel physiological adjustment of the maximal capacity to fix carbon and the cellular carbon quota. On the other hand, normalization by chlorophyll a shows lower values at low growth irradiance reflecting photoacclimation processes. In an opposite fashion, the light limited portion of the curve, when normalized to chlorophyll a, is largely independent of growth irradiance, but varies due to photoacclimation when normalized to carbon. The ubiquitous nature of these relationships for most algal groups has been reviewed by MacIntyre et al. (2002), and several growth and photoacclimation models have been built to match these observations. It results that, to remove an important source of physiological variability, that due to photoacclimation, and to obtain photosynthetic parameters that are independent of growth irradiance, carbon is a better quantity to normalize the light saturated rates and chlorophyll a is better to normalize the light limited part of the curve.

Unfortunately, a direct measure of phytoplankton carbon in situ or from remote sensing does not exist, such that all models of primary productivity published to date use chlorophyll a to normalize both α^{B} and $P^{\mathrm{B}}_{\mathrm{max}}$. Since variability in the biomass-normalized depth-integrated primary production is thought to be mostly driven by the light-saturated rate of photosynthesis (Behrenfeld and Falkowski, 1997), progress in predicting $P^{\mathrm{B}}_{\mathrm{max}}$ is central to estimating oceanic primary production more accurately.

Therefore, if carbon could be measured or estimated accurately, phytoplankton carbon might provide a good alternative for these models. Recently, Behrenfeld and colleagues (Behrenfeld et al., 2005; Behrenfeld and Boss, 2003, 2006) suggested that light scattering could provide an accurate proxy of phytoplankton carbon. These suggestions have brought to the forefront questions regarding the interpretation of these optical parameters. Though it has long been known that the beam attenuation coefficient (c_p, m^{-1}) is a good proxy of the total particulate organic carbon (POC) in case 1 waters (Morel, 1988; Gardner et al., 2006, and references therein), the suggestion of Behrenfeld and Boss (2003) that it represents an accurate proxy of phytoplankton carbon merits further research. In a similar way, the particulate backscattering coefficient (b_{bp}, m^{-1}), which can be obtained from satellite remote sensing, has been used to estimate the concentration of POC (Stramski et al., 1999). More recently, Behrenfeld et al. (2005) based on a good correlation between b_{bp} and chlorophyll a proposed the utilization of the backscattering coefficient to estimate the phytoplankton carbon over large space and time scales. Aware that the sources of backscattered light in the ocean remain unknown (Stramski et al., 2004), we will examine here both b_{bp} and c_p as potential alternatives to Tchl$a$ for constraining the variability of photosynthetic parameters. In this analysis, because measurements of the scattering coefficient (b_p, m^{-1}), are available, we will use them instead of c_p, since c_p is generally used as a surrogate for b_p.

Another proxy of biomass examined herein is phytoplankton absorption ($\bar{a}_{\mathrm{phy}}$, m^{-1}). Indeed it has sometimes been argued that $\bar{a}_{\mathrm{phy}}$ is preferable to Tchl$a$ for studies of primary productivity (Perry, 1994; Lee et al., 1996; Marra et al., 2007). The basis for this proposition is that $\bar{a}_{\mathrm{phy}}$ is more directly linked both to the remote sensing signal and photosynthetic processes than Tchl$a$ (Perry, 1994). The evidence for this suggestion is, however, still lacking on large oceanic scales. Other potentially useful measures examined in this paper are the: photosynthetic absorption ($\bar{a}_{ps}$, m^{-1}) which encompasses all and only the photosynthetic pigments; chlorophyll a fluorescence, which is due to the absorption by all photosynthetic pigments and has the advantage of being readily measured in the ocean with high temporal and spatial resolution but is strongly affected by the physiological state of the algae; and, finally, picophytoplankton biovolume obtained by flow cytometry.

After providing some background to give a mechanistic basis for the interpretation of the photosynthetic parameters, we will use straightforward analyses to verify if any of these biomass proxies can be substituted for Tchl$a$ to obtain better predictions of the phytoplankton photosynthetic parameters. Our study will use a dataset obtained during the BIOSOPE cruise. This cruise encompassed a large range of trophic conditions from the hyperoligotrophic waters of the South Pacific Gyre to the eutrophic conditions associated with the Chile upwelling region, also investigating the mesotrophic HNLC (high nutrient low chlorophyll) waters of the subequatorial region and in the vicinity of the Marquesas Islands. We verify that the relationships obtained are applicable to other regions by comparing our results with those obtained during the PROSOPE cruise which sampled the Moroccan upwelling and the Mediterranean sea.

2 Background

To quantitatively evaluate potential alternatives to Tchl$a$ and interpret them within a more general and fundamental frame, we use the knowledge from theory and laboratory experiments that allows us to describe the photosynthetic parameters before normalization to biomass, that is P_{max} and not $P^{\mathrm{B}}_{\mathrm{max}}$ and α not α^{B}.

The P_{max} depends on the concentration (n_{slowest}, m^{-3}) and the average maximum turnover time ($\bar{\tau}_{\mathrm{slowest}}$, s atoms^{-1}) of the slowest constituent pool in the photosynthetic reaction chain,

$$P_{\mathrm{max}} = 7.174 \times 10^{-17} \frac{n_{\mathrm{slowest}}}{\bar{\tau}_{\mathrm{slowest}}}, \quad (1)$$

where 7.174×10^{-17} mg C atoms^{-1} s h^{-1} is the conversion factor from seconds to hours and mg of carbon to atoms.

Alternatively, $P_{\max}$ can also be related to an instantaneous maximum carbon specific growth rate ($\mu_{\max}$, d^{-1}) realized under saturating irradiance (neglecting respiration and other losses) as $P_{\max}=C_{\text{phy}}\mu_{\max}/DD$, where D is the daylength (hours per day) and C_{phy} the phytoplankton carbon (mg C m^{-3}). This growth rate is an overestimate of the 24-h growth rate since it is valid only under saturating conditions that are not present throughout the day. To analyze our results we will mostly use the representation given in Eq. (1) as it provides a mechanistic explanation of the processes influencing $P_{\max}$.

The two formulations are equivalent since $C_{\text{phy}}\mu_{\max}=cte\left(n_{\text{slowest}}/\bar{\tau}_{\text{slowest}}\right)$, where *cte* is a proportionality constant.

The initial slope of the photosynthesis irradiance curve is given by the product of the spectrally weighted photosynthetic absorption (m^{-1}),

$$\bar{a}_{ps}=\int_{400}^{700} a_{ps}(\lambda)\overset{o}{E}(\lambda)\,d\lambda \Big/ \int_{400}^{700}\overset{o}{E}(\lambda)\,d\lambda, \quad (2)$$

and the maximum quantum yield of carbon fixation for photons absorbed by photosynthetic pigments ($\varphi^{ps}_{\text{C max}}$, mol C [mol photons absorbed]$^{-1}$) as follows:

$$\alpha = 43.2\bar{a}_{ps}\varphi^{ps}_{\text{C max}}. \quad (3)$$

In Eq. (3), the factor 43.2 mg C mol C^{-1} mol photons μmol photons^{-1} s h^{-1} accounts for the conversion from seconds to hours, μmol photons to mol photons, and mg C to mol C.

Thus n_{slowest} and $\bar{a}_{ps}$ are measures of biomass (both scale with the number of cells), the first representing the concentration of slowest molecule in water and the second providing a good proxy of the concentration of pigmented molecule. Therefore, both $P_{\max}$ and α are described by a different "amount" or "biomass" term (n_{slowest} and $\bar{a}_{ps}$), and a term that encompasses variability in the physiological or photosynthetic efficiency ($\bar{\tau}_{\text{slowest}}$ and $\varphi^{ps}_{\text{C max}}$). It follows that, in theory, the best index of phytoplankton biomass for the sake of estimating primary production are n_{slowest} for the light-saturated region of the curve, and $\bar{a}_{ps}$ for the light-limited region of the curve. The exact nature of n_{slowest}, however, remains largely unknown in the ocean (though the RUBISCO enzyme is often considered the slowest pool; Sukenic et al., 1987).

To assess the accuracy with which different proxies of phytoplankton biomass allow us to retrieve the photosynthetic parameters, we will use non-linear regression analyses where we will compare directly $P_{\max}$ and α to proxies of biomass measured in situ. The trend line will provide the average relationship while the variability around the trend line will provide an estimate of the accuracy with which each proxy of biomass retrieves the "biomass component" of $P_{\max}$ and α, namely n_{slowest} and $\bar{a}_{ps}$. The non-linearity of the relationships will allow us to account for second order effects, which would be not easy using normalized values without encountering potential statistical biases (Berges, 1997).

To understand the source of variability around our regression line, it is useful to represent equations 1 and 3 above in terms of normalized quantities. Essentially, the variability around the mean normalized value will be similar to the variability around our regression (because we use non-linear regression with an intercept they are not exactly equivalent). Normalization of $P_{\max}$ to different proxies of phytoplankton biomass (B) leads to $P^{\text{B}}_{\max}=7.174\times10^{-17}\left[\frac{n_{\text{slowest}}}{\text{B}}\right]\frac{1}{\bar{\tau}_{\text{slowest}}}$, and the same normalization for α leads to $\alpha^{\text{B}}=43.2\left[\frac{\bar{a}_{ps}}{\text{B}}\right]\varphi^{ps}_{\text{C max}}$. Since the variability in $\varphi^{ps}_{\text{C max}}$ and $\bar{\tau}_{\text{slowest}}$ should not be related to B, normalization by B removes most of the variability in $P_{\max}$ and α originating from changes in biomass (i.e. making the term in the square brackets nearly constant). Any proxy of biomass that covaries with $\bar{a}_{ps}$ and n_{slowest} will remove some of the variability, but proxies that account for a greater fraction of the variability will perform best. For example, normalizing α by $\bar{a}_{\text{phy}}$ does not account for the variability in the ratio of photosynthetic absorption to total phytoplankton absorption, while normalizing by Tchl*a* leaves the variability in the photosynthetic absorption to Tchl*a*. Table 1 describes the different sources of variability that are not accounted for when a given biomass proxy is used to normalize the photosynthetic parameters. To aid in the interpretation of our results, and to elaborate on Table 1, we address in more detail here the case of the scattering and backscattering coefficients.

The interest of using b_p and b_{bp} as mentioned before lies in their potential for providing information about the phytoplankton carbon biomass. The particulate scattering coefficient is, however, the sum of scattering by all particles. The relative contribution of each particle type depends on their scattering efficiency (which depends on their size, shape, structure, and index of refraction) and on their concentration (Morel and Bricaud, 1986; Morel, 1973). Given a Junge particle distribution of homogenous spherical particles, those in the size range of 0.5 to 20 μm (Morel, 1973) will be the most effective at scattering. In the ocean, we can express the particulate scattering coefficient as $b_p=b_{\text{phy}}+b_{\text{bact}}+b_{\text{het}}+b_{\text{vir}}+b_{\text{min}}+b_{\text{bub}}+b_{\text{org}}$, where b_{phy}, b_{bact}, b_{het}, b_{vir}, b_{min}, b_{bub}, and b_{org} are the contributions from phytoplankton, bacteria, small non-bacterial heterotrophs, viruses, mineral particles, bubbles, and non-living organic matter, respectively. We can thus express the scattering normalized $P_{\max}$ as:

$$P^{b}_{\max}=7.174\times10^{-17}\left(\frac{n_{\text{slowest}}}{b_{\text{phy}}}\right)\left(\frac{b_{\text{phy}}}{b_p}\right)\frac{1}{\bar{\tau}_{\text{slowest}}}$$

a similar equation is obtained for α:

$$\alpha^{b}=43.2\left(\frac{\bar{a}_{ps}}{b_{\text{phy}}}\right)\left(\frac{b_{\text{phy}}}{b_p}\right)\varphi^{ps}_{C\,\text{max}}.$$

Table 1. Summary of sources of variability in the photosynthetic parameters that are not accounted for by the normalization to different biomass proxies (always listed as point #1 below), and the principal origin of this variability (presented below as point #2). See Falkowski and Raven (1997) for details regarding the absorption based proxies; further explanation of the scattering based proxies are developed in the text.

	Absorption-related biomass proxies			
	Tchl*a*	$\bar{a}_{ps}$	$\bar{a}_{\mathrm{phy}}$	Fluorescence
$P_{\max}$	1) ratio: $n_{\mathrm{slowest}}/\mathrm{Tchl}a$. 2) Photoacclimation and nutritional status. Expected to increase with increasing growth irradiance and nutrient availability. Also influenced by species composition.	1) ratio: $n_{\mathrm{slowest}}/\bar{a}_{ps}$. 2) The same sources as Tchl*a*, plus packaging effects and pigment composition. Expected to increase with increasing growth irradiance	1) ratio: $n_{\mathrm{slowest}}/\bar{a}_{\mathrm{phy}}$. 2) The same sources as $\bar{a}_{ps}$.	1) ratio: $n_{\mathrm{slowest}}/\left(\bar{a}_{ps}\varphi_f^{ps}\right)$ where φ_f^{ps} is the quantum yield of fluorescence. 2) Same sources as for $\bar{a}_{ps}$ plus variability due to the quantum yield of fluorescence.
α	1) Chlorophyll specific absorption coefficient ($\bar{a}^*_{ps}$=$\bar{a}_{ps}$Tchl*a*). 2) Pigment composition and packaging, and thus the physiological status and species composition.	1) Physiologically none. 2) Methodologically, it may be susceptible to larger variability than expected due to significant errors in the estimation of $\bar{a}_{ps}$.	1) ratio: $\bar{a}_{ps}/\bar{a}_{\mathrm{phy}}$ 2) Photoacclimatation, nutritional status and species composition. Also affected by errors in the determination of phytoplankton absorption.	1 ratio: $\bar{a}_{ps}/\bar{a}_{ps}\varphi_f^{ps}$ 2) Additional variability in φ_f^{ps} and different measuring irradiance used to "weight" $\bar{a}_{ps}$, and, hence, on the pigment composition.

	Scattering-related biomass proxies		
	b_p (or c_p)	b_{bp}	biovolumes
$P_{\max}$	1) $\left(\frac{n_{\mathrm{slowest}}}{b_{\mathrm{phy}}}\right)\left(\frac{b_{\mathrm{phy}}}{b_{\mathrm{phy}}+b_{\mathrm{bact}}+b_{\mathrm{het}}+b_{\mathrm{vir}}+b_{\mathrm{min}}+b_{\mathrm{bub}}+b_{\mathrm{org}}}\right)$ 2) See text for further details.	1) Same equation as for b_p (replacing b_p by b_{bp}). 2) See text for further details.	1) The intracellular n_{slowest} concentration. 2) Physiological status and species composition. Methodologically limited by the accuracy in volume determination and cellular volumes observed by flow cytometry.
α	1) $\left(\frac{\bar{a}_{ps}}{b_{\mathrm{phy}}}\right)\left(\frac{b_{\mathrm{phy}}}{b_{\mathrm{phy}}+b_{\mathrm{bact}}+b_{\mathrm{het}}+b_{\mathrm{vir}}+b_{\mathrm{min}}+b_{\mathrm{bub}}+b_{\mathrm{org}}}\right)$ 2) See text for further details.	1) Same equation as for b_p (replacing b_p by b_{bp}). 2) See text for further details.	The volume specific absorption coefficient. Dependent on physiological status. Same methodological problems as above.

Therefore, b_p provides a good proxy of phytoplankton biomass for normalizing the photosynthetic parameters if b_{phy} is a good proxy for n_{slowest} or $\bar{a}_{ps}$ (i.e. low natural variability within the first parentheses of the equations above) and if, in addition, it meets one of three requirements (low variability in the second parentheses of above equations): 1) b_p must be mostly influenced by b_{phy} and all other constituents must represent small or negligible contributions to scattering; 2) all other constituents scattering coefficients must covary tightly with b_{phy}; or 3) a combination of the first two conditions leading to a reduced variability in the b_{phy} to b_p ratio.

From monoculture of phytoplankton, we know that b_{phy} is a good measure of phytoplankton carbon; while the carbon per cell shows large variability during the day, the carbon specific attenuation and scattering coefficient remain nearly constant (Stramski et al., 1995; Stramski and Reynolds, 1993; Claustre et al., 2002). The interspecific variability

seems to remain within a factor of ∼5. If b_p is found to be a good estimator of $P_{\max}$, it is however unlikely that it would be affected mainly by the carbon in n_{slowest}, more likely the covariation of n_{slowest} with total phytoplankton carbon would be the cause.

To be a good proxy of phytoplankton biomass, the particulate backscattering coefficient must meet the same three conditions mentioned above for b_p. However, based on Mie theory, particulate backscattering is due to the same constituents as scattering, but the efficiency of backscattering is more strongly weighted towards smaller-size particles (∼0.1 to 1 μm cf., Morel and Ahn, 1991).

3 Materials and methods

All of the data presented herein were collected during the BIOSOPE and PROSOPE cruises. BIOSOPE sampled 2 transects from the Marquesas Islands to Easter Island, and from Easter Island to Concepcion Chile, through the South Pacific Gyre from 26 October to 10 December 2004. PROSOPE sampled the Morocco upwelling and the Mediterranean Sea from 4 September to 4 October 1999 (see Oubelkheir et al., 2005, for cruise track). Because the dataset for the BIOSOPE cruise is more complete and allows consistent analyses between the parameters studied, we carried out the statistical analysis on that dataset only, and used the PROSOPE dataset for comparison purposes only. While we will not discuss the comparison with the PROSOPE dataset further, we will mention here that trends and absolute values compare well with the BIOSOPE dataset for all variables. All the data shown here are obtained from CTD and rosette casts made near solar noon. Nine depths were usually sampled for the PvsE experiments and all data are matched to these depths. For discrete samples obtained from Niskin bottles (e.g. Tchl*a*, PvsE parameters and absorption), we compare data from the same bottle or from duplicate bottles from the same depth as the PvsE curve data. The data obtained from profiling instruments (e.g. CTD, fluorescence, b_p and b_{bp}), are from the same cast as that of the PvsE sample, and represent the average over 2 m centered on the depth of the PvsE bottle.

3.1 Photosynthesis vs. irradiance curves

The PvsE curves of the particulate fraction were determined by closely following the protocol of Babin et al. (1994). One modification was made for the BIOSOPE cruise (but not PROSOPE): we replaced the GFF filters with 0.2 μm pore size polycarbonate membrane filters. This modification reduced the dispersion observed in surface samples (M. Babin, personal observation). Incubations lasted between 2 and 3.5 h. The data were fit to the following equation (Platt et al., 1980; MacIntyre and Cullen, 2005):

$$P = P_s\left[1-\exp\left(-\overset{o}{E}\,\alpha\Big/P_s\right)\right]\left[\exp\left(-\beta\,\overset{o}{E}\Big/P_s\right)\right]+P_o$$

where P_s (mgC m^{-3} h^{-1}) is an hypothetical maximum photosynthetic rate without photoinhibition and an analytic function of β, α and $P_{\max}$; β (mg C m^{-3} h^{-1} [μmol photons m^{-2} s^{-1}]$^{-1}$) is a parameter describing the reduction of the photosynthetic rates due to photoinihibition at high irradiance; and P_o an intercept term. The $P_{\max}$ reported herein are equal to $P_{\max}$+P_o where $P_{\max}$=$P_s\left(\alpha/\alpha+\beta\right)\left(\beta/\alpha+\beta\right)^{\alpha/\beta}$. The 95% confidence interval (CI) on the parameters was estimated using the standard MATLAB routine *nlpredci.m.* Estimated parameters for which the CI was greater than 50% of the parameter value were discarded. To have a uniform dataset, we also discarded the points for which there were no concurrent values for all of the following: Tchl*a*, b_p, b_{bp}, a_{phy}, a_{ps}, and nitrate. This left 159 points for $P_{\max}$ and 153 points for α from an original dataset of 338 PvsE curves. Roughly half of the points (77 for $P_{\max}$ and 75 for α were excluded because of the criteria we chose for the CI. Since the number of phytoplankton biovolume estimates was significantly smaller, data for missing biovolume estimates were not excluded.

3.2 Pigments

The concentration of phytoplankton pigments was measured by HPLC, using a method modified from the protocol of Van Heukelem and Thomas (2001) for the BIOSOPE cruise (Ras et al., 2007), and Vidussi et al. (1996) for the PROSOPE cruise.

3.3 Phytoplankton and photosynthetic absorption

The method used for phytoplankton absorption spectra measurements is detailed in the works of Bricaud et al. (1998) and Bricaud et al. (2004). Photosynthetic absorption was obtained following the procedure of Babin et al. (1996) using the individual pigment spectra in solution given by Bricaud et al. (2004). Both were weighted according to the irradiance inside the photosynthetron (see Eq. 4; the same equation was used for $\bar{a}_{\text{phy}}$ by replacing a_{ps} by a_{phy}) to provide an average value for the spectra.

3.4 Fluorescence

Fluorescence was measured in situ using an Aquatracka III fluorometer (Chelsea Technology Group) placed on the same rosette as the Niskin bottle for the discrete samples. No correction for the decrease of fluorescence due to non-photochemical quenching was attempted and this is expected to increase the variability in the comparison with other biomass proxies.

3.5 Scattering and backscattering coefficient

The particulate scattering (b_p) and backscattering coefficients (b_{bp}) were measured using an AC-9 (WET Labs) and an ECO-BB3 sensor (WET Labs), respectively. AC-9 data were acquired and processed according to the method of Twardowski et al. (1999), using the temperature and salinity correction coefficients obtained by Sullivan et al. (2006). Scattering errors in the reflective tube absorption measurement were corrected using the spectral proportional method of Zaneveld et al. (1994). Between field calibrations with purified water during the cruise, instrument drift was fine-tuned to independent measurements of absorption in the dissolved fraction made on discretely collected samples by (Bricaud et al., 2007)[1]. The ECO-BB3 data were processed according to Sullivan et al. (2005), using the chi-factors obtained therein to convert volume scattering measurements at 117° to backscattering coefficients. For optimal accuracy, direct measurements of in situ dark counts were periodically collected by placing black tape over the detectors for an entire cast. More details on the processing in Twardowski et al. (2007).

3.6 Diffuse attenuation coefficient

The diffuse attenuation coefficient (K_d, m^{-1}) in the visible bands was obtained as described in Morel et al. (2007).

3.7 Phytoplankton biovolumes

Prochlorococcus, *Synechococcus* and picophytoeukaryote biovolumes were estimated from mean cell size and abundance by assuming a spherical shape. See Grob et al. (2007) for details. Cell abundances were directly determined using flow cytometry, except for the weakly fluorescent surface *Prochlorococcus* populations whose abundance was estimated from divinyl chlorophyll *a* concentrations. Mean cell sizes were obtained by establishing a direct relationship between the cytometric forward scatter signal (FSC) normalized to reference beads and cell size measured with a Coulter Counter for picophytoplanktonic populations isolated in situ and cells from culture (see Sect. 2.1 and Fig. 3a in Grob et al., 2007). Mean cell sizes were then used to calculate cell volumes assuming a spherical shape. Finally, biovolumes ($\mu m^3\ ml^{-1}$) were obtained by multiplying cell volume and abundance. Because, as noted above, in surfaces water at some stations, the *Prochlorococcus* population fluorescence was undetectable, we discarded all *Prochlorococcus* measurements for this study. The biovolumes thus include only the *Synechococcus* and picophytoeukaryotes. The maximum cell diameter observed with the instrument settings used during the cruise was 3 μm. This included most of the phytoplankton cells in oligotrophic waters but missed a significant fraction in more eutrophic waters. Similarly, the absence of *Prochlorococcus* may miss a significant fraction of the biomass in oligotrophic waters.

[1]Bricaud, A., Babin, M., Claustre, H., Ras, J., and Tieche, F.: The par titioning of light absorption in South Pacific Waters, in preparation, 2007.

3.8 Stepwise regression and determining the quality of fits

We use three quantities to assess the quality of fits: the correlation coefficient (r), the root mean square error (RMSE), and the mean absolute percent error (MAPE). While the first two are more commonly used statistical measures of fits, the third provides an estimate of variability that is independent of range or absolute values (relative measure, without units) of the data and hence is more easily comparable between different estimated variables. The MAPE is expressed as a fraction (instead of a percentage, sometimes abbreviated as MAE in the literature) and is calculated as $\text{MAPE}=\frac{1}{n}\sum_{i=1}^{n}\left(Y_i-\hat{Y}_i\right)\Big/Y_i$, where Y is the measured data, $\hat{Y}$ is the estimated value and n the total number of points.

All stepwise regressions will be conducted with the following constraints: a variable is added if the maximum p-value is 0.05 and removed if the minimum p-value is 0.10. The p-values provided in the text regarding the stepwise regression are the probability that the regression coefficient is equal to 0.

4 Results and discussion

4.1 Overview of the dataset

This dataset was collected in case 1 waters. In these waters, away from land influences, all the optical properties covary with the phytoplanktonic biomass (which spanned roughly 3 orders of magnitude) as it underlies the functioning of the whole ecosystem. Indeed, an overview of the biomass data collected during the BIOSOPE cruise shows that most variables follow the trends expected as a function of chlorophyll *a* for case 1 waters (Fig. 1); the relationships between surface measurements of b_p, b_{bp}, and a_{phy}, and Tchl*a* concentration are consistent with statistical relationships previously established (Bricaud et al., 2004; Loisel and Morel, 1998; Morel and Maritorena, 2001). It is interesting to note the resemblance between panels A and H showing respectively b_p and the phytoplankton biovolume obtained from the flow cytometry measurements as a function of the Tchl*a* concentration. Despite (or because of) of the lack of *Prochlorococcus* in the biovolumes dataset and the upper limit of 3 μm, and unless strongly covarying particles are present, this suggests that variability in b_p is in large part influenced by the biovolume (similar to carbon concentration) of phytoplankton. A similar observation can be made with respect to $P_{\max}$ and biovolumes which both shows patterns that reassembles strongly those of b_p and suggest that they are good proxy

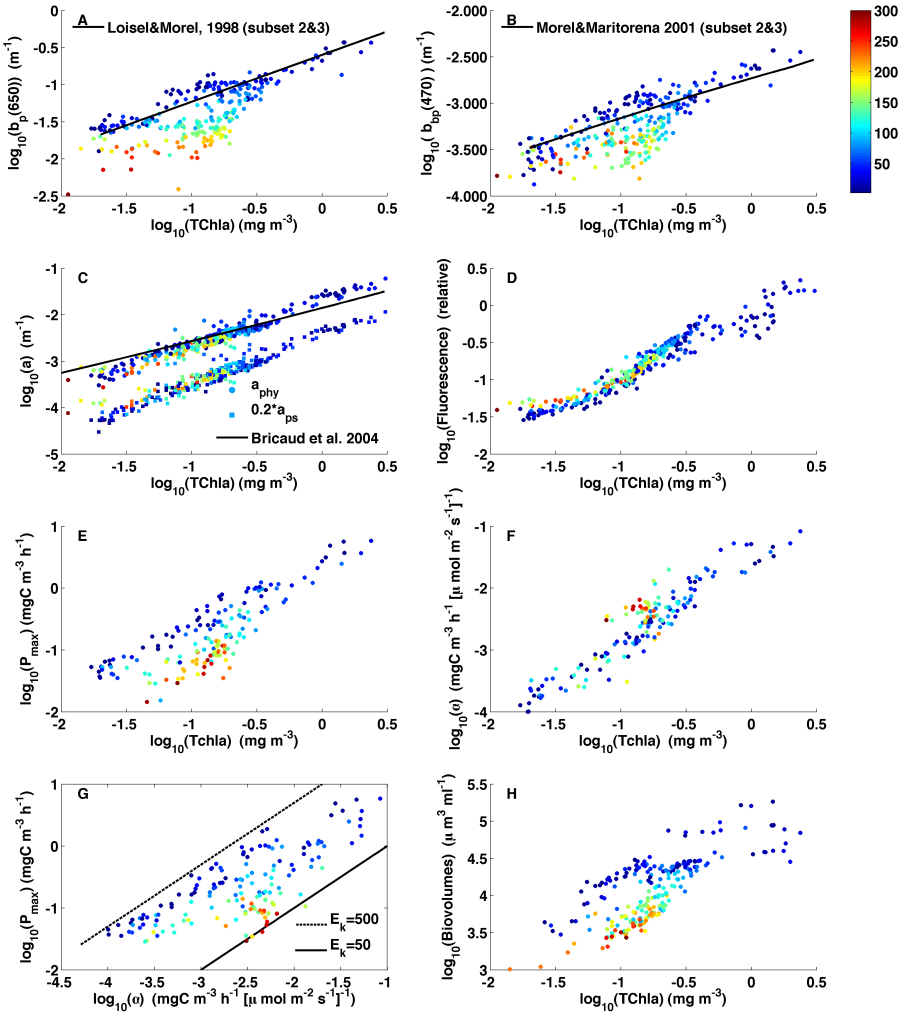

Fig. 1. Comparison of different estimators of phytoplankton biomass obtained during the BIOSOPE cruise with published statistics for case 1 waters. **(A)** Particulate scattering coefficient at 650 nm vs. Tchl*a* (sum of chlorophyll *a* and divinyl chlorophyll (A), **(B)** Backscattering coefficient at 470 nm vs. Tchl*a*, **(C)** Phytoplankton and photosynthetic absorption multiplied by 0.2 (allows it to be discerned from the former) weighted by the photosynthetron irradiance spectra vs. Tchl*a*, **(D)** In situ fluorescence vs. Tchl*a*, **(E)** $P_{\max}$ vs. Tchl*a*, **(F)** α vs. Tchl*a*, **(G)** $P_{\max}$ vs. α, lines are for two extreme saturation irradiances (E_k) for photosynthesis, **(H)** Biovolume obtained from a calibrated flow cytometer vs. Tchl*a*. Colorscale represents depth.

of the slowest pool. The decrease of b_p with depth for a given Tchl*a* concentration (Fig. 1a) is consistent with the oft-reported trends attributed to a "photoacclimation-like" behavior (i.e. an increase in the Tchl*a* per scattering particle, cf. Kitchen et al., 1990). A similar trend is observed in b_{bp} (Fig. 1b). The phytoplankton absorption coefficient (Fig. 1c) generally follows the statistical relationship established for case 1 waters by Bricaud et al. (2004) but shows a slightly higher slope and lower intercept. A sigmoidal shape is observed in log space for the fluorescence vs. Tchl*a* relationship (Fig. 1d). A clear depth dependence is observed in the $P_{\max}$ vs. Tchl*a* relationship, while this dependence is reversed and much less accentuated for α (Figs. 1e and f; see Methods section). The relationship between α and $P_{\max}$ (Fig. 1g) also shows a depth dependence which represents changes in E_k with depth (i.e. higher values at the surface; lower values at depth) consistent with photoadaptation (or less-likely photoacclimation). The predominant factor in these changes of E_k are likely photoadaptation rather than photoacclimation as there is a layering of species with depth in these stratified environments (see Ras et al., 2007).

So while all properties covary with one another, there remains some variability. This remaining variability, however, is not all random (e.g. depth dependence of the b_p vs. Tchl*a* relationship) and thus contains information about the system. If this information is pertinent to the retrieval of photosynthetic parameters some of the measures should provide less variability when compared with the photosynthetic parameters than other.

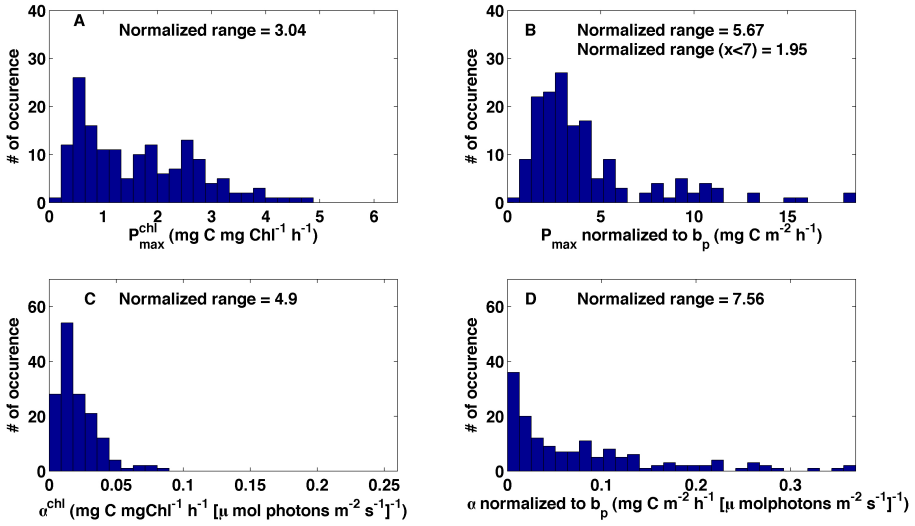

Fig. 2. Histograms of the photosynthetic parameters measured during the BIOSOPE cruise. **(A)** $P^{\mathrm{chl}}_{\mathrm{max}}$, **(B)** P_{max} normalized to b_p, **(C)** α^{chl}, **(D)** α normalized to b_p. The normalized range was calculated as (min(x)–max(x))/median(x), where x is the normalized photosynthetic parameter. It provides a rough guide to compare the variability between the different panels. For panel (B), two ranges are given, one for the whole dataset, as in the other panels, and one for normalized P_{max} smaller than 7 mg C m^{-2} h^{-1} for (focusing on the "normal" region of the distribution). The abscissas are scaled such that the ratio of the maximum of the axis to the minimum value of the data are equal (for each row independently).

Table 2. Statistical difference between the different index of biomass used for predicting P_{max} and α (in Figs. 3 to 6). The estimator for which the correlation coefficient is not different at the 95% confidence level share the same letter. Letters are ordered alphabetically to the quality of the fits (Figs. 3, 4, 5 and 6), the best correlation have an "a" and the worst a "c".

	b_p	Biovolume	Tchl*a*	b_{bp}	a_{phy}	fluorescence	a_{ps}
P_{max}	a	a, b	b	b	b	b	b
α	c	c	a	c	b	a, b	a, b

A comparison of the distributions of the photosynthetic parameters when they are normalized to Tchl*a* or to the particulate scattering coefficient is provided in Fig. 2. The values obtained for $P^{\mathrm{chl}}_{\mathrm{max}}$ [0.26 to 7.2 mg C (mg chl)$^{-1}$ h^{-1}] and α^{chl} [0.0028 to 0.086 mg C (mg chl)$^{-1}$ h^{-1} (μmol photons m^{-2} s^{-1})$^{-1}$] are consistent with values from the literature, but clearly do not cover the full range of variability reported. A review of several datasets of photosynthetic parameters by Behrenfeld et al. (2004) gives a range of 0.04 to 24.3 (mostly between ~0.5 and ~10) mg C (mg chl)$^{-1}$ h^{-1} for $P^{\mathrm{chl}}_{\mathrm{max}}$, and of 0.0004 to ~0.7 (mostly between ~0.005 and ~0.2) mg C (mg chl)$^{-1}$ h^{-1} (μmol photons m^{-2} s^{-1})$^{-1}$ for α^{chl} though some variability in α^{chl} originates from the different spectra used for the measurement irradiance. Using a crude index of dispersion, the normalized range (see Fig. 2 caption for details and the values reported on the graphs), shows that normalization of both P_{max} and α by Tchl*a* reduces the variability in the data relative to normalization by b_p (but only slightly in the case of P_{max}). The distribution for P_{max} normalized to b_p, however, shows a normal distribution of points below values of 7 mg C m^{-2} h^{-1} with a long tail above. If we consider only the points below that threshold, the variability is much reduced and becomes lower than when Tchl*a* is used as the normalization factor. The higher P_{max} normalized to b_p values occur mostly in regions with higher chlorophyll concentrations (coastal upwelling regions, deep chlorophyll maxima, and Marquesas Islands). This could be the result of real physiological variability or indicate a bias in the normalization by b_p with trophic status (e.g. ratio of b_{phy}/b_p increasing with increasing chlorophyll concentration, see Table 1 and Background section).

4.2 Determining the best proxy of phytoplankton biomass to predict photosynthetic parameters

Figures 3 and 4 show the comparison between P_{max} and different measures of biomass. On both figures, the left panels show the scatter plots of P_{max} against the different biomass indices measured, and a 2nd order polynomial obtained on the log-transformed data. The right-hand-side panels show the values of P_{max} predicted by using the polynomial fit against the measured values (the statistics of the fits are also provided). As previously mentioned, all fits and statistics refer only to the BIOSOPE dataset as it is more complete and allows a consistent comparison of all proxies of biomass from an equal number of points taken simultaneously, or near simultaneously, while the PROSOPE dataset is superposed for comparative purposes only. While P_{max} is expected to

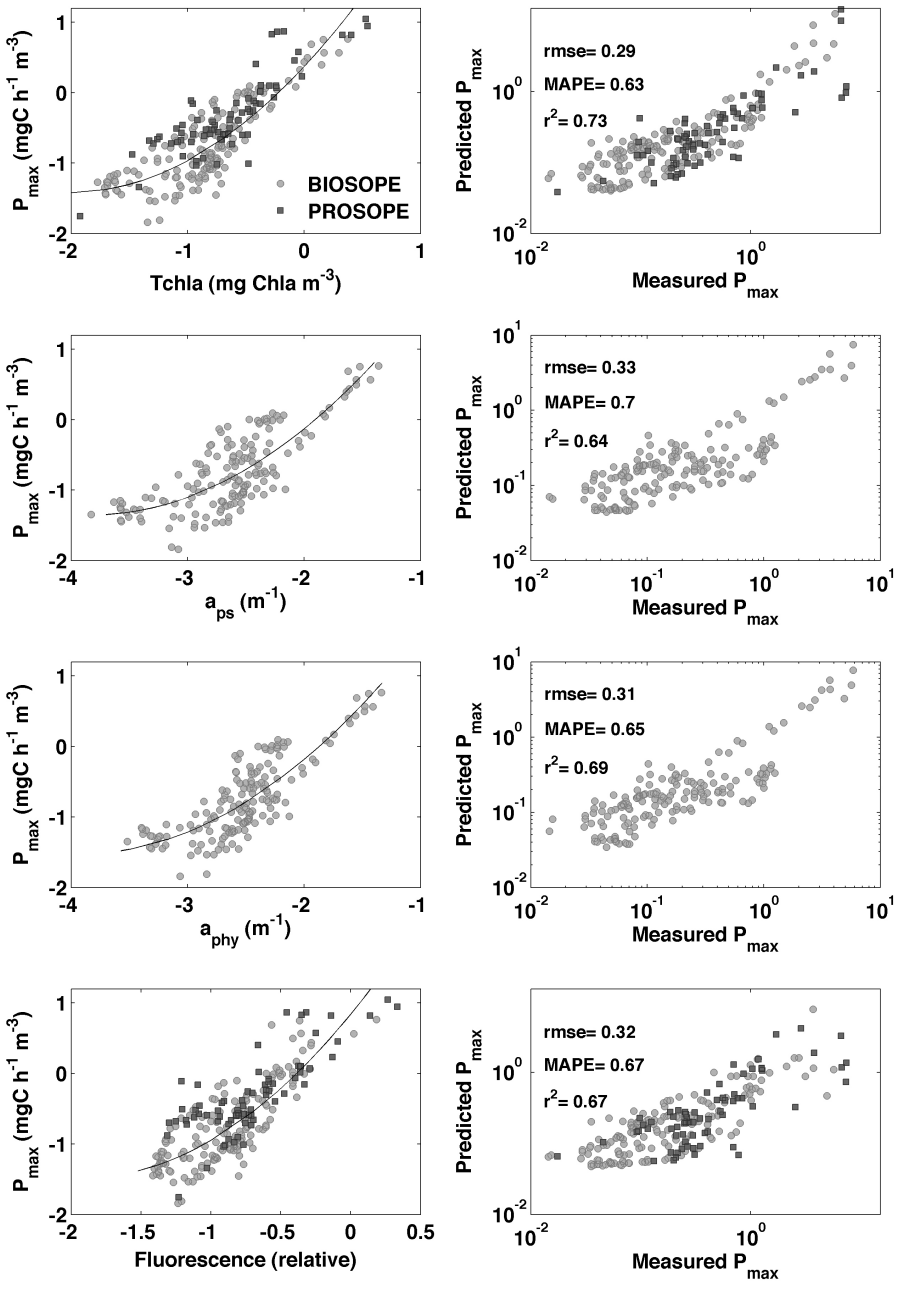

Fig. 3. Relationships between four estimators of biomass and $P_{\max}$. Left Column: $P_{\max}$ vs. the different estimators. The black line represents the best-fit second order polynomial. Right column: Measured and estimated $P_{\max}$ using the best-fit line in the left column. Also shown are the statistics of the predictions.

covary strongly with all proxies of biomass, what interests us here is the remaining variability, which should be lower for the better proxies. Several points can be made about these figures. Firstly, the $b_p(650)$ and biovolumes estimated from flow cytometry measurements provide the best estimates of $P_{\max}$ (Fig. 4). Since the variability in $\bar{\tau}_{\text{slowest}}$ and the measurement errors on $P_{\max}$ are equal for all panels, this suggests that $b_p(650)$ is the best single measure of n_{slowest}. Secondly, the backscattering coefficient provides estimates of $P_{\max}$ that are equivalent to those using Tchl$a$. However, at low values of $P_{\max}$ the predictability is reduced as the slope between $P_{\max}$ and b_{bp} is much smaller (as two become essentially independent). Indeed, for values of $P_{\max} < \sim 0.1$, b_{bp} continues to decrease while $P_{\max}$ remains constant. Thirdly, a_{ps}, a_{phy} and chlorophyll fluorescence all perform similarly in estimating $P_{\max}$ but slightly worse than Tchl$a$. We can summarize

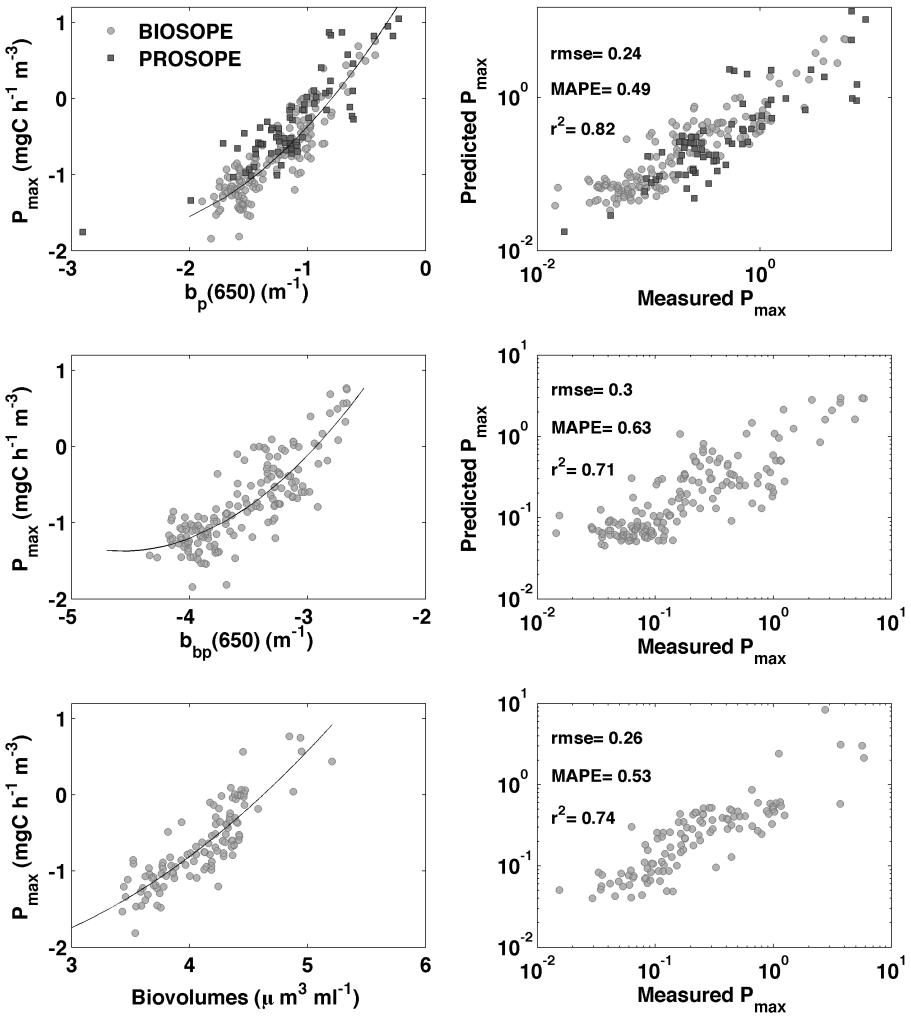

Fig. 4. Relationships between three estimators of biomass and $P_{\max}$. See Fig. 3 for details.

these results in terms of decreasing accuracy of estimates (using MAPE as the index) as follows: $b_p \approx$biovolume$>$Tchl$a$ $\approx b_{bp} \approx$ fluo $\approx a_{\text{phy}} \approx a_{ps}$. Statistically (see Table 2 for a complete comparison), the correlation coefficient (r) on b_p is significantly greater ($p<0.05$, t-test on the z-transform of the correlation coefficient, Sokal and Rohlf, 1995) than the parameters with values of r equal to or lower than that of Tchl$a$ (i.e. Tchl$a$, b_{bp}, fluorescence, a_{phy}, a_{ps}). There is no significant difference between the correlation coefficients on the other parameters.

Figure 5 shows the comparison between α and different measures of biomass. In contrast with the $P_{\max}$ measurements, both measures of scattering as well as the biovolume estimates perform very poorly, while Tchl$a$ and $\bar{a}_{ps}$ show the best estimates, with Tchl$a$ not significantly better than $\bar{a}_{ps}$. Finally, fluorescence is followed by $\bar{a}_{\text{phy}}$. In summary, estimators order as follows (from the most to the least accurate): Tchl$a$ $\approx \bar{a}_{ps} \approx$fluo$>\bar{a}_{\text{phy}} \gg b_p >$ biovolumes $> b_{bp}$. Statistically (see Table 2 for a complete comparison), the correlation coefficient of Tchl$a$ is significantly greater than the other proxies with values of r equal or lower to that of a_{phy} ($p<0.05$; t-test on z-transform). The correlation coefficient on $\bar{a}_{\text{phy}}$ is significantly different from b_p, b_{bp} or biovolumes ($p<0.001$; t-test on the z-transform).

To summarize these results, it can be said that we obtained very intuitive results for the relationships between α and the different proxies of biomass. Indeed, that Tchl$a$, $\bar{a}_{ps}$, and $\bar{a}_{\text{phy}}$ provide the best measures of α is what we expected as they represent a measure closely related to the absorption of photosynthetic pigments. On the other hand, the results concerning $P_{\max}$ are more noteworthy: b_p, despite not being specific to phytoplankton, provides a better estimate of $P_{\max}$ than the traditional measure of Tchl$a$. These results are consistent with those of Behrenfeld et al. (2005); Behrenfeld and Boss (2006) where they showed that the ratio c_p/Tchl$a$ provided good estimates of $P_{\max}$/Tchl$a$. Hence, for the waters studied here, which are representative of many oceanic waters, b_p is the best proxy for estimating $P_{\max}$ when no other

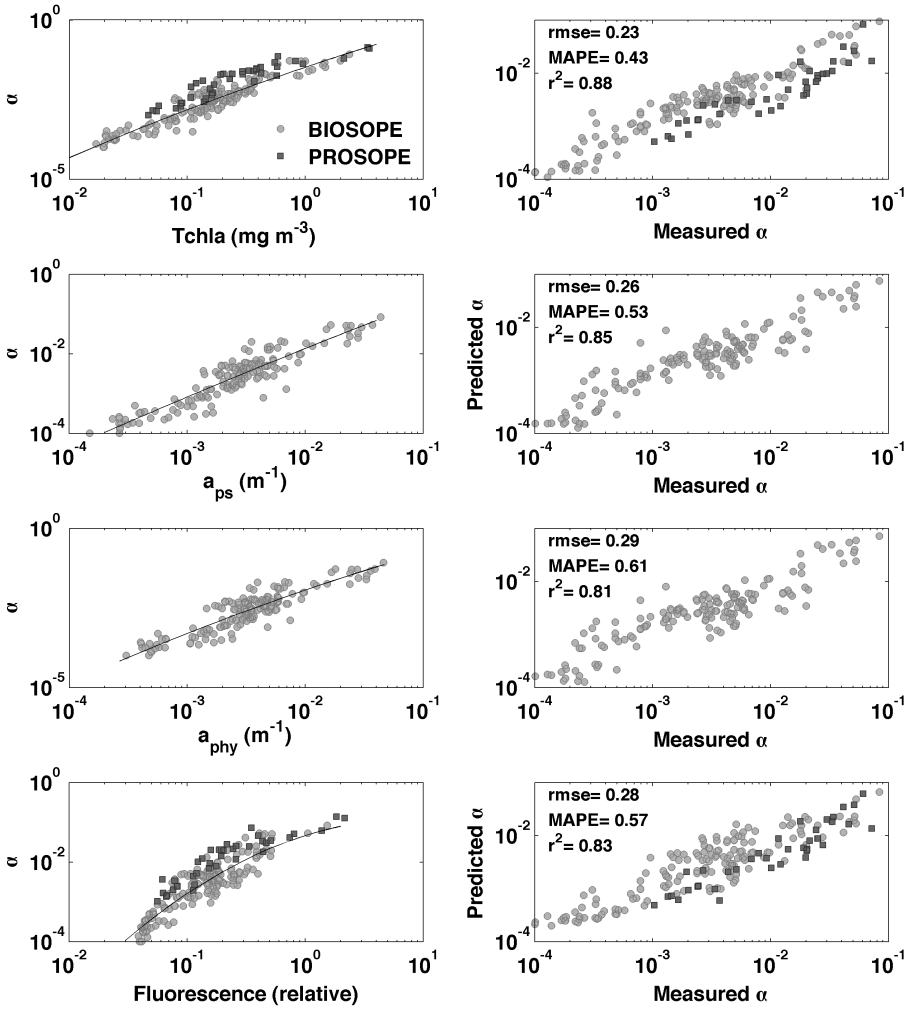

Fig. 5. Relationships between four estimators of biomass and α (in mgC m^{-3} h^{-1} [μmol photon m^{-2} s^{-1}]$^{-1}$). Left Column: α versus the different biomass estimators. The black line represents the best-fit second order polynomial. Right column: Measured and estimated α using the best-fit line in the left column. Also shown are the statistics of the predictions.

measurements are available. This means that b_p is strongly influenced by phytoplankton scattering or that the scattering coefficients of all other particulate matter show tight relationships with the phytoplankton scattering coefficient. Furthermore, since it is better correlated to $P_{\max}$ than Tchl$a$, which is present only in phytoplankton, it implies that b_p provides a measure that covaries better with n_{slowest} than Tchl$a$. Consequently, it implies that there is considerable variability in the ratio n_{slowest}/Tchl$a$ (not correlated with Tchl$a$). Even more interesting is the good retrieval of $P_{\max}$ using $b_{bp}(650)$ which is equivalent to estimates using Tchl$a$. Because the size fractions that are expected to influence b_{bp} the most are smaller than the smallest phytoplankton (assuming a Junge distribution, generally observed during BIOSOPE, Sciandra et al., 2007)[2], it implies that either backscattering from that fraction is very well correlated with phytoplankton backscattering, or phytoplankton cells are affecting b_{bp} more than expected.

We now want to examine the possibility of predicting the large variability in the ratio of n_{slowest}/Tchl$a$ using other environmental variables and examine if the relationship with b_p can be further improved with these same variables.

4.3 Using environmental variables in addition to proxies of phytoplankton biomass

While the results of the previous analysis are interesting, it remains a somewhat academic exercise because biomass proxies are rarely obtained without at least some information about the sampled location and environment. We thus, now turn to our second question. Can we improve the estimates of α and $P_{\max}$ by using additional measurable quantities? In other words, what is the origin of the remaining variability?

[2]Sciandra, A., Stramski, D., and Babin, M.: Variablity in particle size distribution in contrasted trophic regions of the South East Pacific, in preparation, 2007.

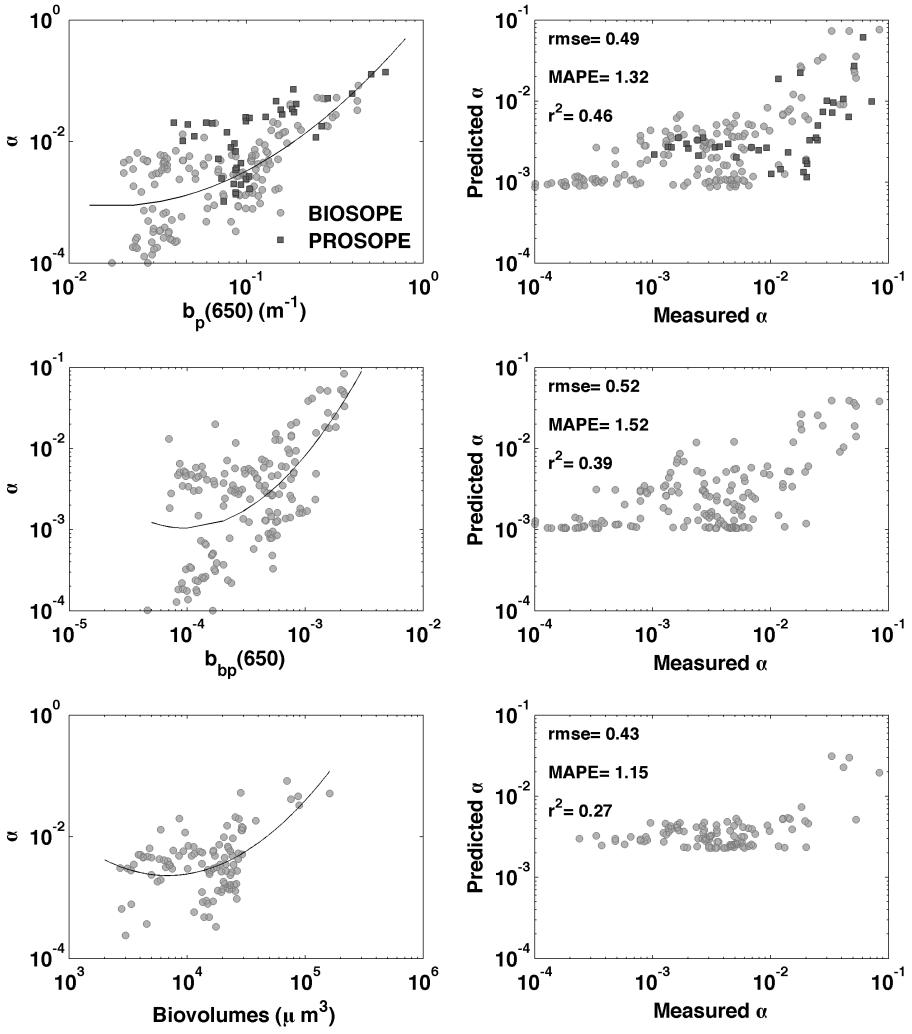

Fig. 6. Relationships between three estimators of biomass and α (in mgC m^{-3} h^{-1} [μmol photon m^{-2} s^{-1}]$^{-1}$). See Fig. 5 for details.

To address this question we used a stepwise regression analysis with the log transform of α and $P_{\max}$ as our dependent variable and a series of potentially relevant independent variables. For each fit, we used only one log-transformed "biomass proxy" (i.e. whether log(Tchl$a$), log(b_p), log(b_{bp})…). The analysis was conducted for all depths. Table 3 provides all the independent variables tested and a summary of the results. A succinct rationale is given for the different variables used (the variables squared allow non-linear relationships to be present). Depth is a general proxy for growth irradiance (including UV), nutrient availability, and mixing regime (while different types of waters were encountered, light, UV and diffusivity coefficient always decrease with depth while nutrient always increase). Temperature is expected to have an effect on enzymatic rates and species composition. The log of the mean PAR irradiance at depth over the last three days provides a measure of irradiance experienced by the cells in their recent past (often referred to as light history), potentially affecting their photoacclimation status. The log of the theoretical PAR irradiance at depth provides a measure essentially similar to the optical depth (except that the surface irradiance is accounted for) and provides a longer term (∼weeks) proxy of the mean irradiance value at depth; relevant to processes of competitive exclusion (by species that have different photoadaptation). The nitrate concentration is used as a proxy of nutrient availability. Figure 7 compares graphically the results for $P_{\max}$ using b_p(650) and Tchl$a$ as the independent biomass variable.

The results are clear (see Table 3, e.g. MAPE row). Using other independent variables beyond biomass, it is possible to significantly improve the relationship between $P_{\max}$ and Tchl$a$ (as well as a_{phy}, a_{ps}, and fluorescence). However, the same does not occur for b_p or b_{bp}, for which the relationships improve only marginally by using several new variables. Most of the improvements using Tchl$a$ arise from

Table 3. Stepwise fit results for P_{max} vs. different indices of biomass. Values represent the fitted coefficients for each variable. NU is used for "Not Used in the fit" (e.g. P_{max}(Tchl$a$)=0.236+1.07log$_{10}$(Tchl$a$)−6.18E−3z+1.35E−5z^2+1.55E−2T).

	Tchl$a$	a_{ps}	a_{phy}	fluo	b_p(650)	b_{bp}(650)
Intercept	0.236	2.42	2.71	0.509	2.05	14.5
Log$_{10}$(Biomass)	1.07	−4.42E−03	−5.39E−3	−6.84E-3	3.21	6.83
Log$_{10}$(Biomass)^2	NU	8.32E−06	1.16E−5	1.61E−5	0.677	0.834
Depth	−6.81E−3	3.34E−2	3.18E−2	NU	NU	NU
Depth^2	1.35E−5	NU	NU	NU	NU	NU
T	1.55E−2	−9.52E−2	NU	NU	NU	−1.95E−1
T^2	NU	1.34E−02	NU	NU	5.36E−3	5.37E−3
Log$_{10}$(E$_{growth}$)†	NU	NU	NU	5.18E−3	NU	NU
Log$_{10}$(PAR$_{theo}$)§	NU	NU	NU	NU	NU	NU
Log$_{10}$(PAR$_{theo}$)^2	NU	1.82	1.93	1.21	−5.55E−3	NU
Log$_{10}$(NO$_3$)	NU	0.143	0.161	NU	NU	NU
RMSE	0.15	0.16	0.16	0.18	0.21	0.25
MAPE	0.29	0.31	0.30	0.36	0.43	0.54
R^2	0.93	0.92	0.90	0.90	0.86	0.80

† E$_{growth}$ is the mean PAR irradiance during daylight (μmol photon m^{-2} s^{-1}) at the sampling depth over the three days previous to the sampling day. It is calculated using the incident irradiance measured on the ship and the attenuation coefficient measured at the station.
§PAR$_{theo}$ is the mean PAR irradiance calculated using the Gregg and Carder (1990) model at the sampling depth using the attenuation coefficient measured at the station for the sampling day. Therefore it does not account for cloudiness.

Table 4. Stepwise fit results for α vs. different indices of biomass. Values represent the fitted coefficients for each variable. NU is used for "Not Used in the fit".

	Tchl$a$	b_p(650)	b_{bp}(650)	a_{ps}	a_{phy}	fluo
Intercept	−1.39	0.63	19.0	1.28	1.36	−1.18
Log$_{10}$(Biomass)	1.36	3.40	767	1.91	1.29	1.47
Log$_{10}$(Biomass)^2	NU	0.652	0.96	0.114	NU	NU
Depth	NU	NU	7.66E−3	NU	−1.12E−2	-3.43E-3
Depth^2	4.81E−6	2.33E−5	5.48E−5	1.22E−5	4.77E−5	2.71E−5
T	NU	NU	−0.642	NU	NU	−1.24E−2
T^2	NU	3.00E−4	1.52E−2	4.64E−4	2.94E−4	NU
Log$_{10}$(E$_{growth}$) †	−3.07E−2	NU	NU	NU	NU	NU
Log$_{10}$(PAR$_{theo}$)§	NU	NU	0.155	NU	NU	NU
Log$_{10}$(PAR$_{theo}$)^2	NU	−1.99E−2	−4.09E−2	NU	−2.29E−2	NU
Log$_{10}$(NO$_3$)	NU	NU	−4.01E−2	NU	−1.167E−2	1.43E−2
RMSE	0.21	0.30	0.31	0.22	0.23	0.21
MAPE	0.40	0.65	0.66	0.44	0.44	0.41
R^2	0.90	0.80	0.78	0.89	0.88	0.90

† See Table 3
§ See Table 3

accounting for the depth effects. This is not unexpected given the clear depth dependence of P_{max} for a given Tchl$a$ concentration observed in Fig. 1e. The relationships retrieved or the parameters used are not discussed further here, but the result that interests us is that the pigment or absorption based estimates of P_{max} can be relatively easily improved beyond a simple biomass relationship whereas the same is not true for the scattering based methods. The latter hence have lower predictive skill when other sources of variability are accounted for. We also note that the errors on the prediction of P_{max} using this simple regression approach with Tchl$a$ are very reasonable; the average error (MAPE) is 25% for the BIOSOPE dataset (see Table 3) and 33% for the independent PROSOPE dataset.

We carried out a similar analysis for α (Table 4 and Fig. 8). In this case, all estimates improved by important margins

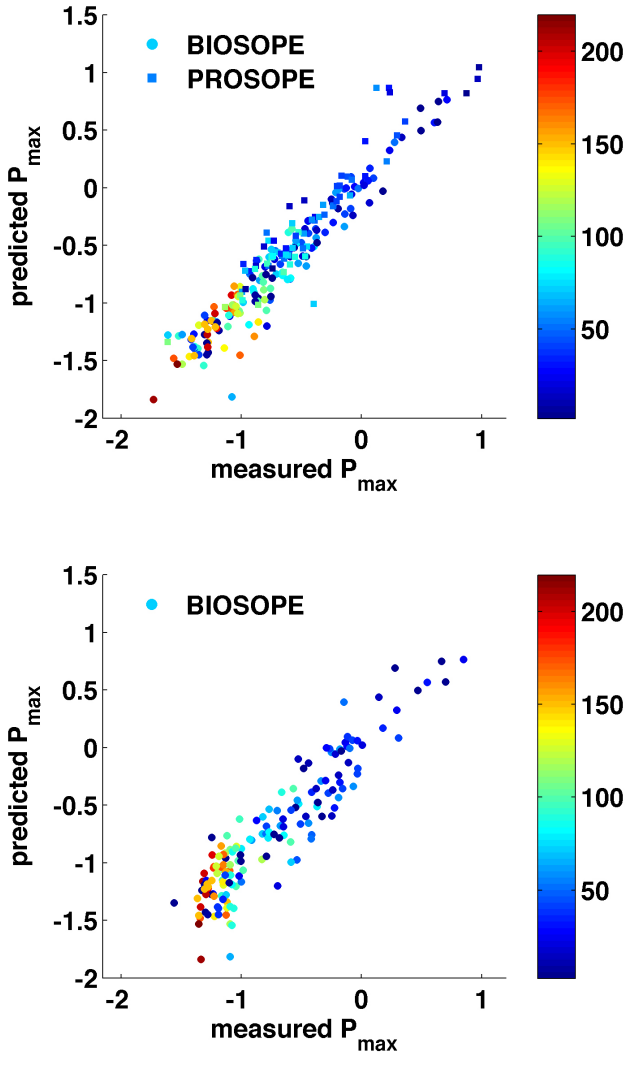

Fig. 7. Prediction of $P_{\max}$ using several variables. **(a)** Using Tchl*a* as the biomass index and other variables as given in Table 3. **(b)** Same as (a) except using b_p as the biomass proxy.

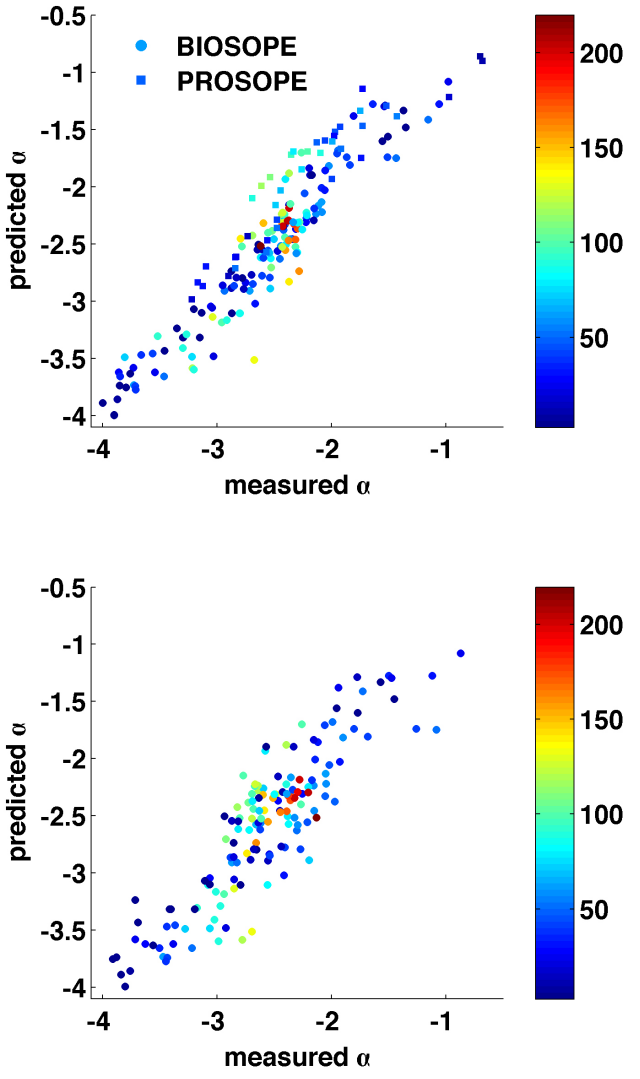

Fig. 8. Prediction of α (in $\mathrm{mgC\,m^{-3}\,h^{-1}}$ [μmol photon $\mathrm{m^{-2}\,s^{-1}}$]$^{-1}$) using several variables. **(a)** Using Tchl*a* as the biomass index and other variables as given in Table 4. **(b)** Same as (a) except using b_p as the biomass proxy.

relative to the relationship using only the biomass index. However, the Tchl*a* and absorption based measures remained significantly better than the scattering based methods (Table 4). In fact, the improvements in the scattering based methods are due to the fact that they started off so poorly, and any variable that is somewhat correlated with α or Tchl*a* will improve the relationships.

4.4 Additional information in scattering beyond Tchl*a*

An important question remains: given the regression using Tchl*a* and environmental variables, can scattering based variables allow us to improve estimates of $P_{\max}$ and α? In other words, is there supplementary information in the scattering based proxies? This question can also be addressed by a stepwise regression analysis, by verifying if adding scattering based measures improves the fit significantly. We tested the addition of the following variables: $b_p(650)$, $b_p(650)^2$, and Tchl$a/b_p(650)$. Only the $b_p(650)$ provided a very small but significant improvement to the fits for $P_{\max}$ (RMSE decreased from 0.1488 to 0.1441). None provided significant improvements in the regression of α (all had values of $p > 0.14$). We therefore conclude that, for the waters studied, the bulk scattering measurements adds very little to the estimates of photosynthetic parameters, once basic information regarding chlorophyll concentration and irradiance at depth is available (see Tables 3 and 4).

This conclusion is of course only valid for the environments and the space and time scales that we studied. Scattering based measurements have been proposed to help in the estimation of primary production based on diurnal changes in the c_p (e.g. Siegel et al., 1989; Claustre et al., 2007) or of phytoplankton carbon concentration and growth rate from space on large spatial scales (Behrenfeld et al., 2005). These applications are beyond the scope of our analysis and our results are difficult to extrapolate to them.

4.5 Estimation of primary productivity using empirical relationships

Primary productivity models are generally expressed with the production (P)-irradiance relationship normalized to biomass (e.g. P^{B}). This relationship is depth integrated and then multiplied by biomass, $P{=}BP^{\mathrm{B}}$ (the depth integration can occur after the multiplication by biomass if depth photosynthetic parameters vary with depth). In order to reduce the variability in P^{B}, some authors relate it to its location and time (Platt and Sathyendranath, 1999; Longhurst, 1998), while others describe it in terms of environmental variables (e.g. P^{B} (T, Salinity, E_d)) (Behrenfeld and Falkowski, 1997). The aim of our study is to identify the normalization factor ("B") that reduces as much as possible the variability in the photosynthetic parameters. In doing so, we obtain regressions that predict $P_{\max}$ and α from different biomass proxies and environmental variables (Table 3 and Table 4). Our relationships can thus be written as $P{=}f(B,\ T,$ Salinity, $E_d,\ z\ldots)$. Therefore, these relationships, or extensions of them, could be used in primary production models using remote sensing data, but without the need to multiply the resulting primary production by an estimate of the phytoplankton biomass. Here, the phytoplankton biomass serves directly as a predictive variable.

5 Conclusions

Within the context of evolving ocean observation technology, our analysis consolidates a rationale for the direction taken over the past 50 years or so for estimating primary productivity. Indeed, we find that chlorophyll *a* remains the best proxy of phytoplankton biomass for studies of primary productivity. In particular, we find that the scattering coefficient (and other scattering-based variables) did not provide information about the photosynthetic parameters that could not be more accurately estimated by a measure of chlorophyll *a* (or fluorescence) and incident irradiance at depth. This is probably due as much to the superior accuracy of the estimation of Tchl*a* compared to other measurements as to its specificity to phytoplankton. There is one main limitation in our present study: most of our dataset originates from subtropical stratified waters (BIOSOPE) and warm temperate waters (PROSOPE). Photosynthetic parameters depend on environmental variables and thus on the regions sampled. While our measurements are representative of a wide range of chlorophyll concentrations (from $\sim$0.02 to $\sim 3\,\mathrm{mg\,m^{-3}}$), they are not representative, for example, of polar or cold temperate water columns. It is possible that in these waters scattering-based measurement prove to be more robust for the determination of phytoplankton photosynthetic parameters.

Acknowledgements. D. Tailliez and C. Marec are warmly thanked for their efficient help in CTD rosette management and data processing. We also want to thank F. Tièche for processing the phytoplankton absorption data, P. Raimbault, J. Ras and A. Morel for providing the nutrient, HPLC and irradiance data. This is a contribution of the BIOSOPE project of the LEFE-CYBER French program. This research was funded by the Centre National de la Recherche Scientifique (CNRS), the Institut des Sciences de l'Univers (INSU), the Centre National d'Etudes Spatiales (CNES), the European Space Agency (ESA), the National Aeronautics and Space Administration (NASA) and the Natural Sciences and Engineering Research Council of Canada (NSERC). Y. Huot was funded by postdoctoral scholarships from NSERC (Canada) and CNES (France). C. Grob was supported by CONICYT (Chili) through the FONDAP Program and a graduate fellowship, and by the ECOS-CONICYT Program.

Edited by: E. Boss

References

Babin, M. and Morel, A.: An incubator designed for extensive and sensitive measurements of phytoplankton photosynthetic parameters, Limnol. Oceanogr., 39, 694–702, 1994.

Babin, M., Morel, A., Claustre, H., Bricaud, A., Kolber, Z., and Falkowski, P. G.: Nitrogen- and irradiance-dependent variations of the maximum quantum yield of carbon fixation in eutrophic, mesotrophic and oligotrophic marine systems, Deep-Sea Res. Pt I, 43, 1241–1272, 1996.

Behrenfeld, M. J. and Falkowski, P. G.: A consumer's guide to phytoplankton primary productivity models, Limnol. Oceanogr., 42, 1479–1491, 1997.

Behrenfeld, M. J. and Boss, E.: The beam attenuation to chlorophyll ratio: An optical index of phytoplankton physiology in the surface ocean?, Deep-Sea Res. Pt I, 50, 1537–1549, 2003.

Behrenfeld, M. J., Prasil, O., Babin, M., and Bruyant, F.: In search of a physiological basis for covariations in light-limited and light-saturated photosynthesis, J. Phycol., 40, 4–25, 2004.

Behrenfeld, M. J., Boss, E., Siegel, D. A., and Shea, D. M.: Carbon-based ocean productivity and phytoplankton physiology from space, Global Biogeochem. Cy., 19, GB1006, doi:1010.1029/2004GB002299, 2005.

Behrenfeld, M. J. and Boss, E.: Beam attenuation and chlorophyll concentration as alternative optical indices of phytoplankton biomass, J. Mar. Res., 64, 431–451, 2006.

Berges, J. A.: Ratios, regression statistics, and "Spurious" Correlation, Limnol. Oceanogr., 42, 1006–1007, 1997.

Bricaud, A., Claustre, H., Ras, J., and Oubelkheir, K.: Natural variability of phytoplankton absorption in oceanic waters: Influence of the size structure of algal populations, J. Geophys. Res.-Oceans, 109, C11010, doi:11010.11029/12004JC002419, 2004.

Claustre, H., Bricaud, A., Babin, M., Bruyant, F., Guillou, L., Le Gall, F., Marie, D., and Partensky, F.: Diel variations

in prochlorococcus optical properties, Limnol. Oceanogr., 47, 1637–1647, 2002.

Claustre, H., Huot, Y., Obernosterer, I., Gentili, B., Tailliez, D., Lewis, M.: Gross community production and metabolic balance in the South Pacific Gyre, using a non intrusive bio-optical method, Biogeosciences Discuss., 4, 3089–3121, 2007, http://www.biogeosciences-discuss.net/4/3089/2007/.

Falkowski, P. G. and Raven, J. A.: Aquatic photosynthesis, First ed., Blackwell Science, Malden, 375 pp., 1997.

Gardner, W. D., Mishonov, A., and Richardson, M. J.: Global poc concentrations from in-situ and satellite data, Deep-Sea Res. Part II, 53, 718–740, 2006.

Gregg, W. W. and Carder, K. L.: A simple spectral solar irradiance model for cloudless maritime atmosphere, Limnol. Oceanogr., 35, 1657–1675, 1990.

Grob, C., Ulloa, O., Claustre, H., Huot, Y., Alarcon, G., and Marie, D.: Contribution of picoplankton to the total particulate organic carbon concentration in the eastern South Pacific, Biogeosciences, 4, 837–852, 2007, http://www.biogeosciences.net/4/837/2007/.

Kitchen, J. C., Ronald, J., and Zaneveld, V.: On the noncorrelation of the vertical structure of light scattering and chlorophyll a in case I waters, J. Geophys. Res.-Oceans, 95, 20 237–20 246, 1990.

Lee, Z. P., Carder, K. L., Marra, J., Steward, R. G., and Perry, M. J.: Estimating primary production at depth from remote sensing, Appl. Optics, 35, 463–474, 1996.

Loisel, H. and Morel, A.: Light scattering and chlorophyll concentration in case 1 waters: A reexamination, Limnol. Oceanogr., 43, 847–858, 1998.

Longhurst, A. R.: Ecological geography of the sea, Academic Press, San Diego, 398 pp., 1998.

MacIntyre, H. L. and Cullen, J. J.: Using cultures to investigate the physiological ecology of microalgae, in: Algal culturing techniques, edited by: Anderson, R. M., Academic Press, 2005.

Marra, J., Trees, C. C., and O'Reilly, J. E.: Phytoplankton pigment absorption: A strong predictor of primary productivity in the surface ocean, Deep-Sea Res. Pt I, 54, 155–163, 2007.

Morel, A.: Diffusion de la lumière par les eaux de mer. Resultats expérimentaux et approche théorique., AGARD lectures series, 3.1.1–3.1.76, 1973.

Morel, A. and Bricaud, A.: Inherent properties of algal cells including picoplankton: Theoretical and experimental results, in: Photosynthetic picoplankton, edited by: Platt, T. and Li, W. K. W., Canadian bulletin of fisheries and aquatic sciences, 521–559, 1986.

Morel, A.: Optical modeling of the upper ocean in relation to its biogenous matter content (case 1 waters), J. Geophys. Res.-Oceans, 93, 10 749–10 768, 1988.

Morel, A. and Ahn, Y.-H.: Optics of heterotrophic nanoflagellates and ciliates: A tentative assessment of their scattering role in oceanic waters compared to those of bacterial and algal cells, J. Mar. Res., 49, 177–202, 1991.

Morel, A. and Maritorena, S.: Bio-optical properties of oceanic waters: A reappraisal, J. Geophys. Res.-Oceans, 106, 7163–7180, 2001.

Morel, A., Gentili, B., Claustre, H., Babin, M., Bricaud, A., Ras, J., and Tieche, F.: Optical properties of the "Clearest" Natural waters, Limnol. Oceanogr., 52, 217–229, 2007.

Oubelkheir, K., Claustre, H., Sciandra, A., and Babin, M.: Bio-optical and biogeochemical properties of different trophic regimes in oceanic waters, Limnol. Oceanogr., 50, 1795–1809, 2005.

Perry, M. J.: Measurements of phytoplankton absorption other than per unit of chlorophyll a, in: Ocean optics, edited by: Spinrad, R. W., Carder, K. L., and Perry, M. J., Oxford monographs on geology and geophysics, Oxford University Press, New York, 107–116, 1994.

Platt, T., Gallegos, C. L., and Harrison, W. G.: Photoinhibition of photosynthesis in natural assemblages of marine phytoplankton, J. Mar. Res., 38, 687–701, 1980.

Platt, T. and Sathyendranath, S.: Spatial structure of pelagic ecosystem processes in the global ocean, Ecosystems, 2, 384–394, 1999.

Ras, J., Claustre, H., and Uitz, J.: Spatial variability of phytoplankton pigment distributions in the Subtropical South Pacific Ocean: comparison between in situ and predicted data, Biogeosciences Discuss., 4, 3409–3451, 2007, http://www.biogeosciences-discuss.net/4/3409/2007/.

Siegel, D. A., Dickey, T. D., Washburn, L., Hamilton, M. K., and Mitchell, B. G.: Optical determination of particulate abundance and production variations in the oligtrophic ocean, Deep-Sea Res., 36, 211–222, 1989.

Sokal, R. R. and Rohlf, F. J.: Biometry the principles and practice of statistics in biological research, 3 ed., W.H. Freeman and Company, New York, 887 pp., 1995.

Stramski, D. and Reynolds, R. A.: Diel variations in the optical properties of a marine diatom, Limnol. Oceanogr., 38, 1347–1364, 1993.

Stramski, D., Shalapyonok, A., and Reynolds, C. S.: Optical characterization of the marine oceanic unicellular cyanobacterium synechococcus grown under a day-night cycle in natural irradiance, J. Geophys. Res.-Oceans, 100, 13 295–13 307, 1995.

Stramski, D., Reynolds, C. S., Kahru, M., and Mitchell, B. G.: Estimation of particulate organic carbon in the ocean from remote sensing, Science, 285, 239–242, 1999.

Stramski, D., Boss, E., Bogucki, D., and Voss, K. J.: The role of seawater constituents in light backscattering in the ocean, Prog. Oceanogr., 61, 27–56, 2004.

Sukenic, A., Bennett, J., and Falkowski, P. G.: Light-saturated photosynthesis – limitation by electron transport or carbon fixation, Biochim. Biophys. Acta, 891, 205–215, 1987.

Sullivan, J. M., Twardowski, M. S., Zaneveld, J. R., Moore, C., Barnard, A., Donaghay, P. L., and Rhoades, B.: The hyperspectral temperature and salinity dependencies of absorption by water and heavy water in the 400–750 nm spectral range, Appl. Optics, 45, 5294–5309, 2006.

Twardowski, M. S., Sullivan, J. M., Donaghay, P. L., and Zaneveld, J. R.: Microscale quantification of the absorption by dissolved and particulate material in coastal waters with an ac-9, J. Atmos. Ocean. Tech., 16, 691–707, 1999.

Twardowski, M. S., Claustre H., Freeman, A., Stramski, D., and Huot, Y.: Optical backscattering properties of the "clearest" natural waters, Biogeosciences Discuss., 4, 2441–2491, 2007, http://www.biogeosciences-discuss.net/4/2441/2007/.

Zaneveld, J. R. V., Kitchen, J. C., and Moore, C. C.: The scattering error correction of reflecting tube absorption meters, Ocean Optics XII, 44–55, 1994.